Global Topography of Transition Zone Discontinuities from SS Underside Reflection and P-to-s Conversion Data Sets.

B. Tauzin, E. Debayle and G. Wittlinger

Ecole et Observatoire des Sciences de la Terre, Université Louis Pasteur, Strasbourg, France

Transition zone discontinuities and geodynamics

We focus on phase transitions of olivine mineral in the transition zone of the mantle, the so-called 410 and 660 km depth discontinuities.

The 410-km discontinuity is generally thought to be caused by the phase transformation of low-pressure olivine (α-phase) to wadsleyite (β-phase) and the 660-km discontinuity by the phase transformation of ringwoodite (γ-phase) to perovskite and magnesiowüstite. These phase changes with opposite Clapeyron slopes induce a temperature dependent thickness of the transition zone which may be an indicator for lateral heat fluctuations in the mantle.
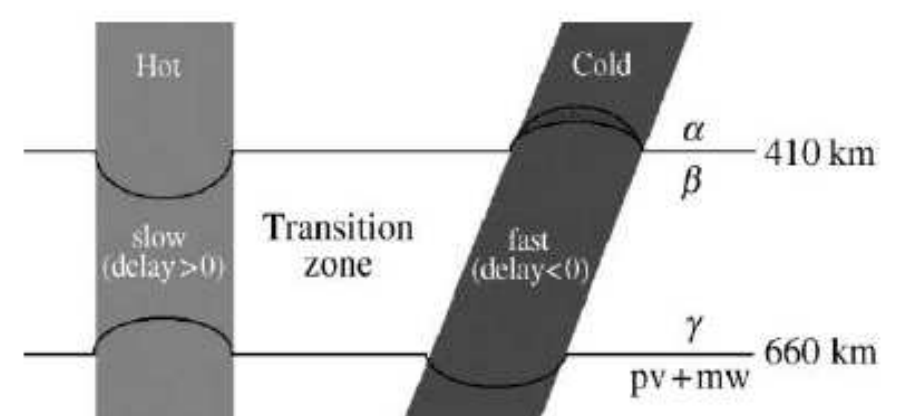
Figure 1, schematic illustration of thermal control of olivine phase transformations in the transition zone showing perturbations to transition zone thickness (from [1]).

Infering the thickness of the transition zone is only influenced by these thermal dependences (actually, chemical heterogeneities also affect the discontinuities), an increased (decreased) thickness of 13 km would be expected for a 100°K negative (positive) anomaly (**Figure 1**). Correlations between depth of 410 and 660 km discontinuities would be interpreted as a dominant effect of chemical heterogeneity or non-olivine component phase transformations.

Data and Processing

Figure 2, To achieve a global coverage of the Earth, we use two complementary data sets : P-to-s conversions at depth d (Pds) under the stations give major constraints under continents whereas SS reflexions at depth d (SdS) are less sensitive to station repartition and reduce the lack of information under oceans. See ray diagrams for Pds conversions (left) and SdS reflexions (right) at both 410 et 660 km depth discontinuities. Epicentral distances are 45° and 80° for conversions and 110° and 180° for reflexions.
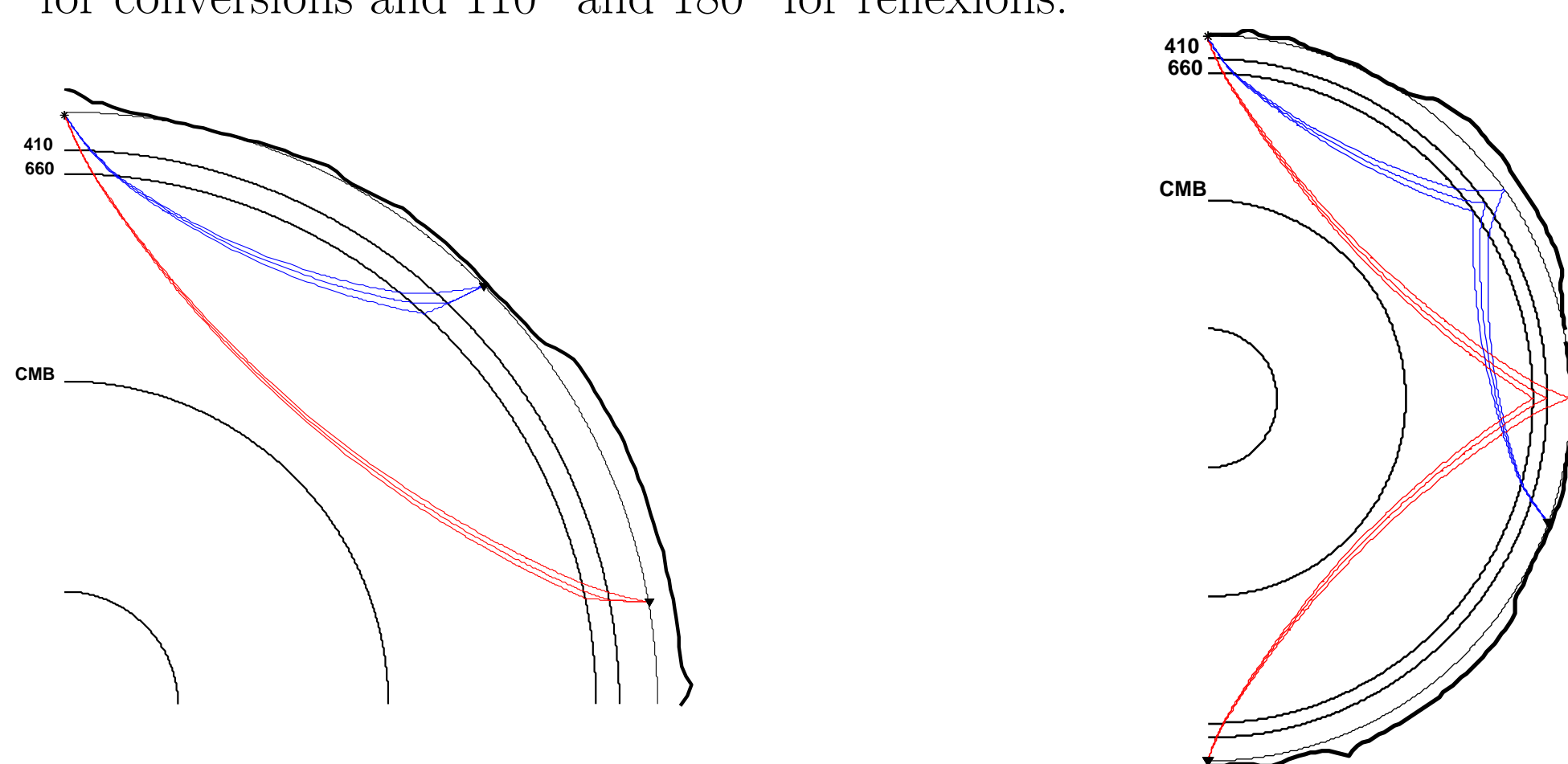
DATA SELECTION & PROCESSING	P-to-s	SS
No. of Stations	86	172
No. of Events	2475	1862
Mag. range (all type)	6-9.9	6-9.9
Distance range (°)	45-90	110-180
Filtering (s)	5-100	15-100
No. Usable Traces	26350	20476

We first remove the analogic response of each instrument to replace it by the 20 October 2000 response of *Geoscope* station PAF. Then, two distinct sequences of processing are applied on each data-set.

• **P-to-s conversions**

We rotate components toward the theoric directions of P, Sv, Sh energy of propagation. Strict P-to-s reflectivity is difficult to identify on the Sv component because of conversions of waveforms of the coda of the P-wave. We apply a similar method to Ligorrìa and Ammon (1999) [2] deconvolving P energy from the Sv component. The deconvolution is iterative with spike positions being determined by cross-correlation of the P wave-train with Sv component. Given the spike positions and the P reference waveform, we form by convolution a first order seismogam that we fit to the residual seismogram of previous iteration. Using a least square criterion, the process stops when an additional spike fails to improve fit to the data significantly.

• **SS reflexions**

We rotate horizontal components to obtain Sh polarized energy on transverse component. Then traces are aligned on the maxima of a cross correlation with a SS reference pulse.

The global data sets

Figure 3 and 4, left (**a.**), Sv (Sh) synthetic reflectivity for a source at 30 km depth in IASP91 [3]. Right (**b.**), stack of all data sets by ranges of 0.5° epicentral distances. Averaging (stacking) large numbers of seismograms yields signals from precursor and converted phases which are to small to be observed in individual traces. Red are positive amplitudes and blue negative ones. Seismograms are aligned on P (SS) reference phase at $t = 0s$. Black Pds, PcP and SdS hododchrons are computed by ray tracing through the model.
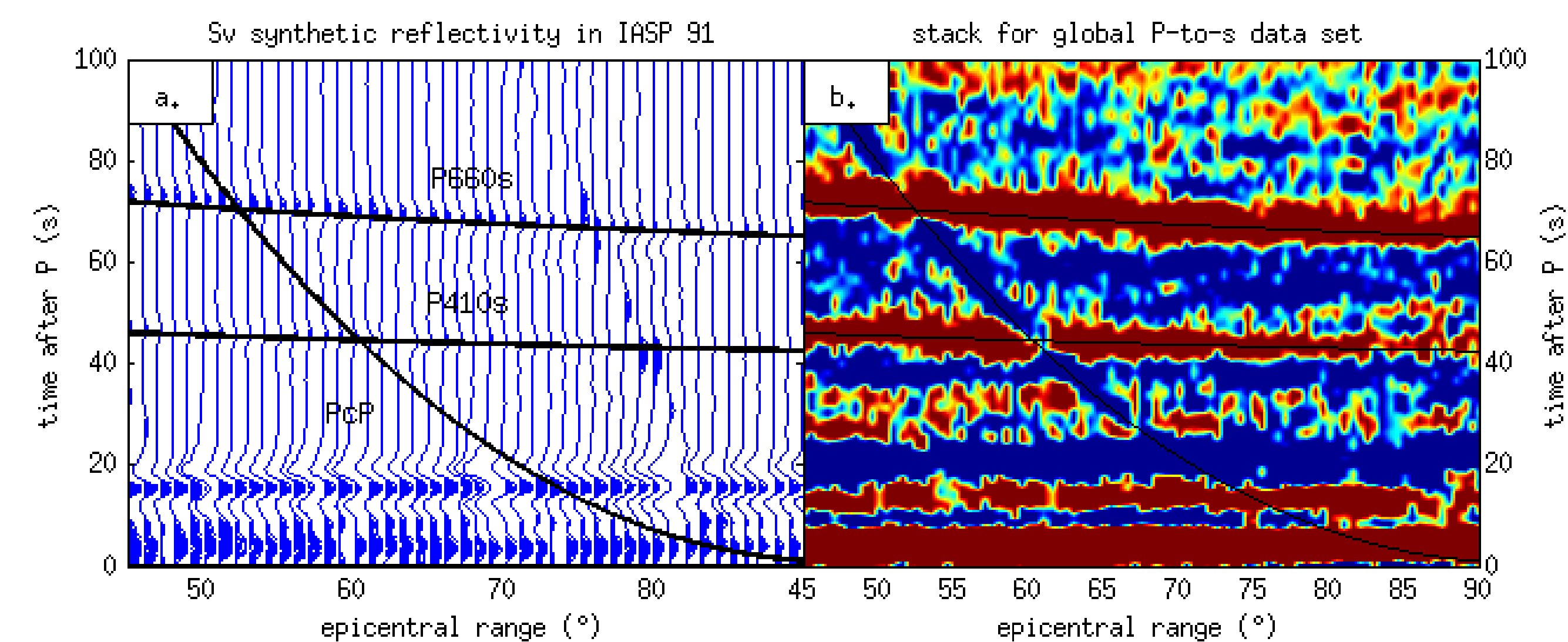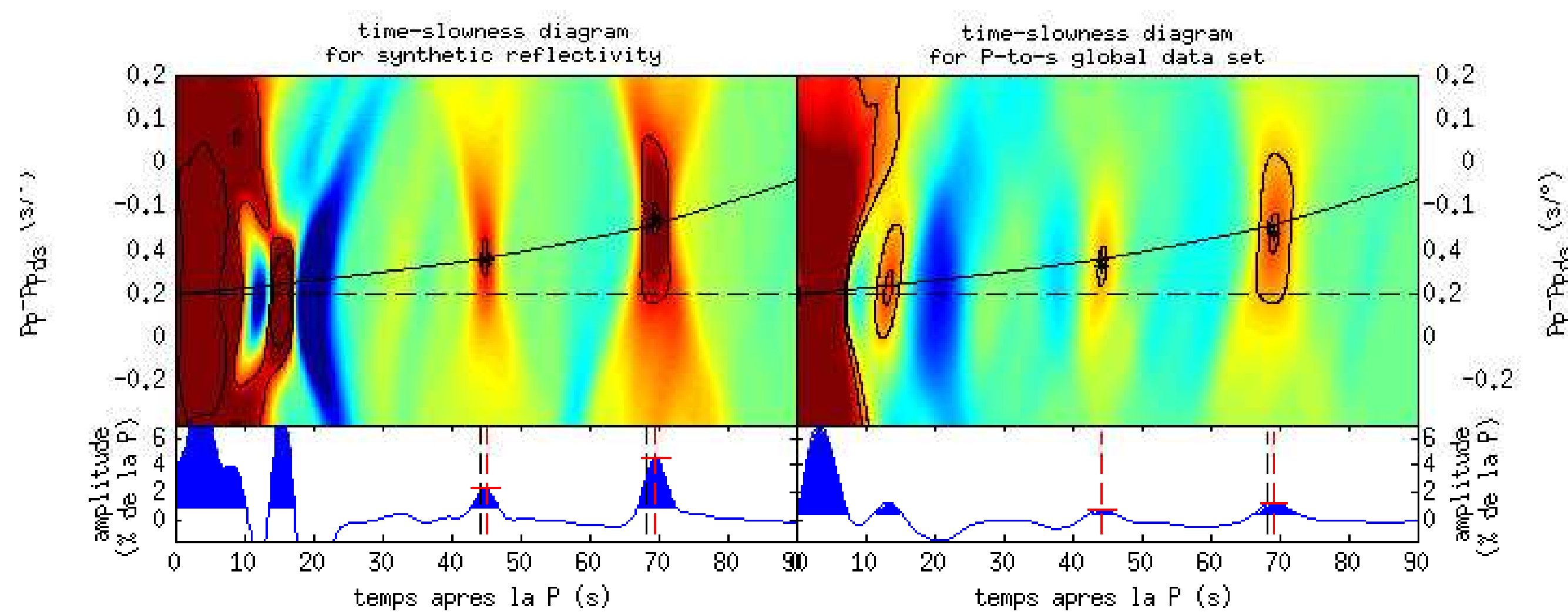
figure 5 and 6, Move-out corrections for SS-precursors (P-to-s conversions) are obtained by stacking all seismograms (receiver functions) in the time-slowness domain (upper cadran).

For P-to-s conversions, we directly pick maximum amplitudes corresponding to 410-km and 660-km conversions on the time-slowness diagram. Black crosses and black stars in upper pictures are theoric and observed slowness-time for the phases.
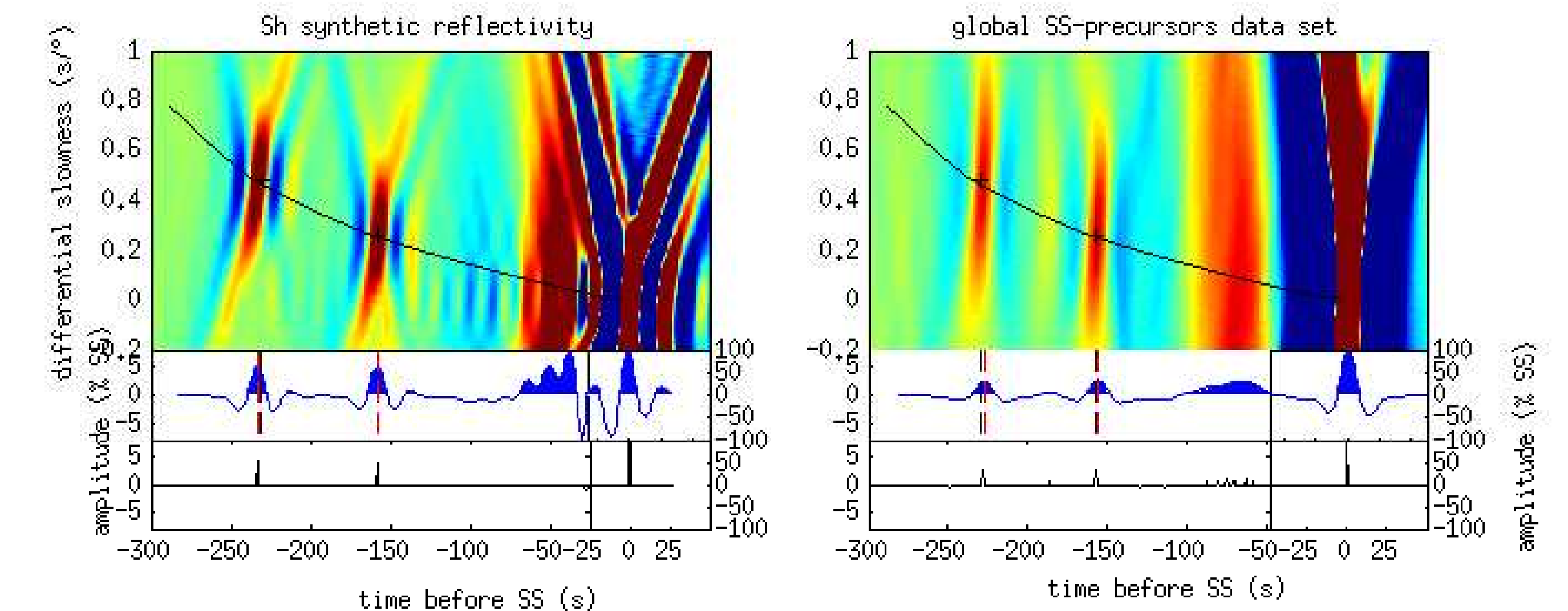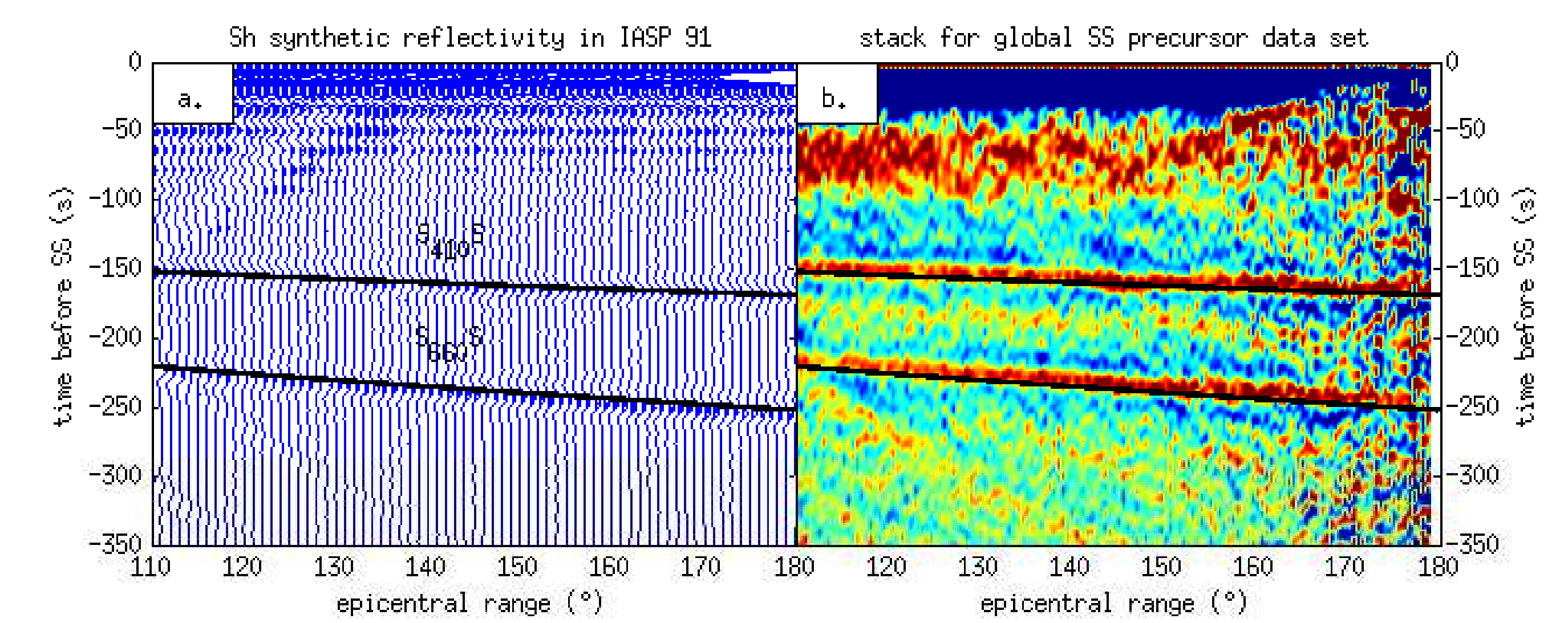
For SS-precursors, slant stacks are converted to single traces based on the expected slowness and arrival time of precursor phases (black curvatures) in IASP91 velocity model. Blue traces (middle) are recovered amplitudes on the curvature. Theoric and observed differential times appear respectively as dashed vertical black and red lines. We make iterative deconvolution to obtain accurate values of differential travel times (bottom).

Global transition zone thickness

$P-Pds$ and $SdS-SS$ differential travel times are converted to conversion/reflexion depth from travel times of these phases in IASP91, without corrections for transition zone structure.
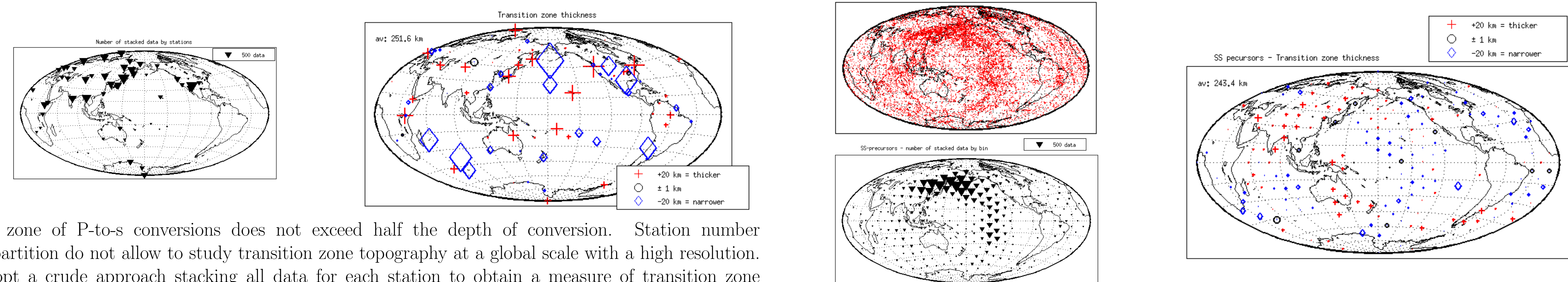
Fresnel zone of P-to-s conversions does not exceed half the depth of conversion. Station number and repartition do not allow to study transition zone topography at a global scale with a high resolution. We adopt a crude approach stacking all data for each station to obtain a measure of transition zone thickness under the station.

Fresnel zone for SS-reflexions is broader (about 10°). For these reason, we stack the data in 362 caps of approximately 10° radius.

Our maps present the same major features than other studies : an important thickening under north-west Pacific and a narrowing in central Pacific. Mean thickness obtained from SS-precursors (243 km) is slighty superior than results from previous studies (242 km). Our mean thickness for transition zone obtained with converted waves (251 km) agree more with results of Chevrot et al (1999) [4] rather than a more recent study of Lawrence (2006) [5] (242 km). Lawrence explains that plane wave-front approximation used by Chevrot may be at the origine of an overestimation of the global transition thickness (8km). Without corrections for transition zone velocity structure, it is presently difficult to corroborate one of the two studies.

References

[1] Bina, C.R., Treatise on Geochemistry, vol 2, 39-59, Elsevier Science Publishing.

[2] Ligorrìa, J. and Ammon, C., Bull. Seismol. Am., vol 85, 1395-1400, 1999.

[3] Kennett, B.L.N., Iaspei 1991 seismological tables, Res. Sch. of Earth Sci. Int., Aust. Nat. Univ., Canberra, 1991.

[4] Chevrot, S., Vinnik, L.P and Montanger, J.P, Global-scale analysis of the mantle Pds phases, J. Geophys. Res., vol 101, 20203-20219, 1999.

[5] Lawrence, J.F. and Shearer, P.M., A Global Study of Transition Zone thickness using Receiver Functions, J. Geophys. Res., in press, 2006.